Published in final edited form as:
J Immunol. 2011 June 15; 186(12): 6925–6932. doi:10.4049/jimmunol.1100211.

HIV-1 reduces Aβ-degrading enzymatic activities in primary human mononuclear phagocytes[1]

Xiqian Lan[*], **Jiqing Xu**[*], **Tomomi Kiyota**[*], **Hui Peng**[*], **Jialin C. Zheng**[*], and **Tsuneya Ikezu**[*,†,‡]

[*]Department of Pharmacology and Experimental Neuroscience, University of Nebraska Medical Center, Omaha, NE 68198-5880, USA

[†]Department of Pharmacology and Experimental Therapeutics, Boston University School of Medicine, Boston, MA 02118, USA

Abstract

The advent and wide introduction of antiretroviral therapy (ART) has greatly improved the survival and longevity of HIV-infected patients. Unfortunately, despite ART treatment, these patients are still afflicted with many complications including cognitive dysfunction. There is a growing body of reports indicating accelerated deposition of amyloid plaques, which are composed of amyloid-β peptide (Aβ), in HIV-infected brains. Though how HIV viral infection precipitates Aβ accumulation is poorly understood. It is suggested that viral infection leads to increased production and impaired degradation of Aβ. Mononuclear phagocytes (macrophages and microglia) that are productively infected by HIV in brains play a pivotal role in Aβ degradation through the expression and execution of two endopeptidases: neprilysin (NEP) and insulin-degrading enzyme (IDE). Here we report that NEP has the dominant endopeptidase activity towards Aβ in macrophages. Further, we demonstrate that monomeric Aβ degradation by primary cultured macrophages and microglia was significantly impaired by HIV infection. This was accompanied with great reduction of NEP endopeptidase activity, which might be due to the diminished transport of NEP to cell surface and intracellular accumulation at the endoplasmic reticulum and lysosomes. Therefore, these data suggest that malfunction of NEP in infected macrophages may contribute to acceleration of beta amyloidosis in HIV-inflicted brains and modulation of macrophages may be a potential preventative target of Aβ-related cognitive disorders in HIV-affected patients.

Keywords

HIV infection; mononuclear phagocytes; neprilysin; Aβ clearance

Introduction

The antiretroviral therapy (ART) has shown significant advancement in the longevity of HIV-infected patients. The affected populations are facing the new challenges of age-related complications, including diabetes, cancer, atherosclerosis, psychiatric disorders, and cognitive dysfunctions leading to senile dementia (1-3). The pathogenesis of HIV-related brain injury may intersect with Alzheimer's disease (AD) in several aspects, including accumulation of amyloid-β peptide in the brain, activation of brain mononuclear phagocytes, dysfunction of the blood-brain barrier, glial inflammation, and metabolic disorders (4).

[1]This work was supported in part by NIH grants R01MH083523, R21 AG032600, R01MH072539 (TI), and P01 NS043985 (TI, JZ).

[‡]To whom correspondence should be addressed: Tel: 617-414-2658; tikezu@bu.edu.

Meanwhile, there is a growing body of evidence showing that brain amyloid deposition is increased in HIV infected patients, though the extent and relation of this deposition to the clinical state and regional HIV infection remain unresolved (1). In addition, it has been reported that Aβ amyloidosis is accelerated in the brains of patients undergoing highly active antiretroviral therapy (HAART), which is probably the result of a number of adverse effects inflicting HAART-medicated patients. These adverse effects are known as AD risk factors, such as immune reconstitution syndrome, lypodystrophic and metabolic effects causing hyperlipidemia, alterations in body fat distribution to metabolically inactive areas, diabetes, and coronary artery disease (5-7). However, how HIV infection or HIV infection in conjunction with HAART medication precipitates Aβ accumulation is largely unknown.

A significant body of evidences suggests that Aβ accumulates in AD is the result of an imbalance between Aβ production and Aβ clearance (8-10). Normally, Aβ, generated via sequential proteolysis of amyloid precursor protein (APP), in the central nervous system (CNS) can be cleared via protease-mediated proteolysis or efflux to general circulation through the neurovascular systems (for review, see (8, 11, 12)). Macrophages and microglia, which are the predominant cells productively infected with HIV in the brain (13, 14), have been shown to play major roles in internalization and degradation of Aβ (15, 16). Macrophages, the peripheral counterpart to microglia, have attracted much attention recently based on the findings that a subset of microglia surrounding and attempting to clear Aβ-containing plaques in transgenic AD mouse models are bone marrow derived (17-19). Bone marrow-derived microglia, but not resident microglia, have been reported to prevent the formation and even eliminate brain amyloid deposits (18). However, there is little known about how HIV infection affects the capability of macrophages to catabolize Aβ. It is suggested that HIV infection together with normal aging can accelerate amyloid accumulation by both increasing Aβ production and impairing Aβ degradation (3). Further, pro-inflammatory cytokines, which are upregulated in the HIV-infected brains, can stimulate neurons to promote Aβ production (20-23).

On the other hand, HIV infection may cause a faulty Aβ degradation by macrophages and microglia, contributing to Aβ accumulation. Macrophages and microglia express two major Aβ-degrading endopeptidases, namely neprilysin (also called neutral endopeptidase and enkephalinase, CD10, NEP, EC 3.4.24.15) (24, 25) and insulysin (insulin degrading enzyme, IDE, EC 3.4.24.56) (26). NEP appears to be the predominant protease that degrades Aβ in the brain (27-30). NEP is a type II membrane-bound zinc metalloendopeptidase localized primarily on the plasma membrane with its catalytic site exposed extracellularly (hence an ecto-peptidase), making this peptidase a prime candidate for peptide degradation at extracellular sites of amyloid accumulation. Numerous studies have implicated NEP as a rate-limiting Aβ degrading enzyme in the brain (25, 31, 32). Expression levels of the Aβ-binding scavenger receptors; scavenger receptor A (SRA), CD36, and RAGE (receptor for advanced-glycosylation end products), and IDE, neprilysin, and matrix metalloprotease (MMP)-9 are decreased twofold to fivefold in microglia in the aged brain of an AD mouse, compared to their littermate controls (33). NEP and IDE become inactivated and down-regulated during both the early stages of AD and aging (34-36).

It was reported that HIV viral protein Tat-derived peptide inhibited NEP activity *in vitro*, and recombinant Tat added directly to brain cultures resulted in a 125% increase in soluble Aβ (37, 38). Nevertheless, HIV encodes at least nine proteins, so it will be more pathophysiologically relevant to examine the effect of the complete HIV viral infection on macrophage- and microglia- mediated Aβ catabolism. In this report we examined whether Aβ clearance via degradation and the enzymatic activity of NEP in mononuclear phagocytes, both brain perivascular macrophages and microglia, is altered as a result of HIV infection. Our *in vitro* study demonstrates that HIV infection significantly impaired Aβ degradation in

mononuclear phagocytes. Further, we confirmed that NEP exhibits the dominant endopeptidase activity towards Aβ degradation in mononuclear phagocytes. However, we found that HIV viral infection dramatically compromised NEP activity, but not NEP expression level, which was concomitant with significant reduction in the cell surface level of NEP protein and intracellular NEP accumulation in the endoplasmic reticulum and lysosomes.

Materials and Methods

Cell culture

Isolation and cultivation of monocytes were performed as previously reported (39). Briefly, human monocytes were recovered from peripheral blood mononuclear cells (PBMC) of HIV-1 and hepatitis B seronegative donors after leukopheresis and purified by countercurrent centrifugal elutriation (40). Monocytes were cultured in Medium A containing DMEM (Invitrogen, Carlsbad, CA, USA) supplemented with 10% heat-inactivated human serum, 2 mM L-glutamine (2 mM), gentamicin (50 μg/mL), ciprofloxacin (10 μg/mL), and M-CSF (1000 U/mL, R&D Systems, Minneapolis, MN, USA). Monocytes were cultivated in Medium A for 7 days allowing their differentiation into macrophages, which were then referred to as monocyte-derived macrophages (MDM). MDM were maintained in Medium B, which is Medium A without M-CSF. Human microglia were isolated following the described protocols (39, 41, 42). Fetal brain tissue (gestational age, 14 to 16 weeks) was obtained from the Birth Defects Laboratory, University of Washington, (Seattle, WA, USA), in full compliance with the ethical guidelines of the NIH and the Universities of Washington and Nebraska Medical Center. At least 3 different donors were tested for the experiments using MDM and microglia.

Viral infection

MDM cultured in plates or on cover slips (intended for cell staining) were rinsed twice with 1X PBS, then incubated for 24 hours with either Medium B alone in the case of the control group or with Medium B containing HIV-1_{pYu2} (titrated as 1 pg HIV p24 protein per cell, NIH AIDS Research & Reference Reagent Program, Germantown, MD, USA) in the infected group (43). Then cells were washed three times with 1X PBS and replaced with Medium B, monitored for cytopathic effects by nuclear staining of apoptotic cells and maintained for 3, 7 or 10 days.

Aβ degradation in MDM and microglia

Primary cultured MDM or microglia were plated onto 96-well plates. Viral infection was carried out as above. Briefly, solid Aβ peptide (Aβ 1-42, Invitrogen) was dissolved in cold hexafluoro-2-propanol (HFIP, Sigma-Aldrich, St. Louis, MO, USA) and incubated at room temperature for 1 hour. The HFIP was then removed by evaporation, and the resulting peptide was stored as a film at −20 °C. The resulting film was dissolved in anhydrous DMSO (Sigma-Aldrich) at 250μM, and then diluted at 10μM in Medium B. MDM were infected with HIV-1_{pYu-2}, and at three days post infection (dpi) the cells were incubated with 10μM Aβ for 1 hour, then fixed with freshly depolymerized 4% paraformaldehyde for 15 minutes. Standard immunofluorescence was performed using anti-Aβ specific antibodies NU-2 (1:100 dilution; mouse monoclonal kindly provided by Dr. William Klein at Northwestern University, Evanston, IL, USA) or 6E10 (1:1000 dilution, mouse, Covance Resaerch Product, Princeton, NJ), and Alexa Fluor®488-conjugated anti-mouse IgG (H+L) (Molecular Probes/Invitrogen) secondary antibody. Cells were counterstained with Hoechst 33342 (1:2000 dilution, Invitrogen) and subjected for immunofluorescence microscopy and fluorescent intensity measurement.

Cellular NEP and IDE endopeptidase activity assay

MDM maintained in Medium B for 3 to 7 days were rinsed twice with ice-cold PBS, then lysed in lysis buffer (20 mM Tris-Cl pH 7.4, 0.5% trition X-100, 10% sucrose, 1 μg/mL aprotinin, and 10 μM phenylmethane sulfonyl fluoride, all from Sigma-Aldrich). The lysates were centrifuged at 15,000 × g for 15 minutes at 4°C, and protein concentrations of the supernatants were measured by standard BCA assay, using the BCA Protein Assay Kit (Thermo Scientific, Rockford, IL, USA).

Endopeptidase activities were assayed in a 96-well plate. In each well, 10 μg lysate and 10 μM fluorogenic peptide Mca-RPPGFSAFK(Dnp)-OH (R & D systems) were mixed in reaction buffer (100 mM Tris-Cl pH 7.5, 50 mM NaCl, 10 μM $ZnCl_2$), and incubated in the dark for 1 hour at 37°C. Insulin (10 μM, Invitrogen), a potent competitive inhibitor of IDE towards Aβ, or thiorphan (10 μM, Sigma-Aldrich), a specific NEP inhibitor, was added to distinguish specific enzyme activities in the cell lysates. Fluorescent intensity of the cleaved fragments was measured by fluorometry with excitation at 320 nm and emission at 405 nm. IDE activity was defined as the activity sensitive to insulin inhibition; while NEP activity was defined as the activity sensitive to thiorphan inhibition.

Immunocapture-based NEP endopeptidase activity assay

Goat anti-human NEP antibody (2 μg/mL) (AF1182, R & D systems) diluted in sodium bicarbonate (100 mM, pH 9.0) was coated on Nunc MaxiSorp 96-well plates (Thermo Scientific) overnight at 4°C. The plates were washed 6 times with PBS containing 0.5% Tween-20 and non-specific binding of antibody was blocked by incubation with 1% PBS-bovine serum albumin (Sigma-Aldrich) for 3 hours at room temperature. Plates were then washed 6 times with PBS containing 0.5% Tween-20. MDM lysates (200 μg) or microglia lysates (100 μg) were added to the coated plates and incubated at 4°C overnight. After washing 6 times, the fluorogenic peptide (10 μM) diluted in reaction buffer (100 mM Tris-Cl pH 7.5, 50 mM NaCl, 10 μM $ZnCl_2$) was added and incubated at 37°C in the dark for 1 hour, then fluorescence was measured with excitation at 320 nm and emission at 405 nm.

Effect of HIV viral proteins on endopeptidase activities of recombinant IDE and NEP

HIV-1 Tat protein (Cat# 2222) and HIV-1 gp120 (Cat# 7363) were obtained from NIH AIDS Research & Reference Reagent Program. Tat protein (0.1, 1, 10 μg/mL) or gp120 (1, 10, 100 μM) was mixed with 20 ng recombinant human IDE (R & D systems) or 10 ng recombinant human NEP (R & D systems) in reaction buffer with shaking at room temperature for 10 minutes. This was followed by the addition of 10 μM fluorogenic peptide as described and incubated at 37°C in the dark for 1 hour. Fluorescence was measured with excitation at 320 nm and emission at 405 nm.

Immunoblotting

Macrophage lysates were prepared as mentioned above. Protein concentrations were determined using the BCA Protein Assay Kit (Thermo Scientific). Protein (25 μg) was electrophoresed on 10% SDS-PAGE and transferred to Immuno-Blot PVDF membranes (Bio-Rad, Hercules, CA, USA), followed by incubation in blocking buffer (5% skim fat milk in TBST) for 1 hour at room temperature. Membranes were then incubated overnight at 4°C with primary antibodies against IDE (1:500 dilution; rabbit polyclonal, PC730, EMD Chemicals, Gibbstown, NJ, USA), NEP (1:100 dilution; mouse monoclonal, NCL-CD10-270, Novocastra/Leica Microsystems, Bannockburn, IL, USA), and β-actin (1:40,000 dilution; mouse monoclonal, AC-15, Sigma-Aldrich). Subsequently, membranes were incubated with horseradish peroxidase-conjugated secondary anti-rabbit or anti-mouse secondary antibodies (1:10,000 dilution; Jackson ImmunoResearch Laboratories, West

Grove, PA, USA) for 1 hour at room temperature. Immunoreactive bands were visualized by enhanced chemiluminescene (GE Healthcare Biosciences, Piscataway, NJ, USA) and captured with CL-X Posure Film (Pierce). For data quantification the films were scanned with a CanonScan 9950F scanner (Canon USA, Inc., Lake Success, NY); the acquired images were then analyzed on a Macintosh computer using the public domain NIH image program (http:rsb.info.nih.gov/nih-image/).

Immunofluorescence

MDM were seeded onto 15 mm cover slips housed in 24-well plates. Seven days after infection, cells were fixed with 4% paraformaldehyde (PFA, Sigma-Aldrich) and immunocytochemistry was conducted as reported (44). Briefly, in order to visualize plasma membrane-localized NEP, fixed cells were not permeabilized prior to incubation with blocking buffer containing 5% BSA and 5% normal donkey serum in PBS for 1 hour at room temperature. Afterwards, samples were incubated overnight with p24 antibody (1:50 dilution in PBS; mouse monoclonal, M0857, Dako North America, Inc, Carpinteria, CA, USA) and NEP antibody (1: 50 dilution in PBS; goat polyclonal, R&D Systems) at 4°C, followed by washing with PBS for three times. Then samples were incubated for 30 minutes at room temperature with appropriate fluorescent-labeled secondary antibodies (for p24, Alexa Fluor 647 donkey anti-mouse IgG; for NEP, Alexa Fluor 488 donkey anti-goat IgG) diluted 1:500 in PBS. After washing with PBS for three times, cells were also incubated for 20 minutes at room temperature with Alexa Fluor 594-conjugated phalloidin (1:40, Invitrogen) to visualize filamentous actin cytoskeleton and with Hoechst 33342 (1:5000, Invitrogen) to stain nuclear DNA. Images were acquired using a laser scanning confocal microscope (510 Meta, Carl Zeiss MicroImaging, LLC, Thornwood, NY, USA) at an objective of 40X and a 2X zoom view for the interested area. To stain NEP within all cellular compartments, cell staining followed the above procedures except that cells were permeabilized with 0.5% Triton-X-100 for 15 minutes at room temperature prior to blocking for non-specific binding. The average fluorescence intensity for NEP, phalloidin, and Hoechst 33342 was measured per region of interest (ROI) for each group (15 fields per group), and the intensity value was normalized by the number of cells as determined by the Hoechst 33342 staining as per 100 cells. Normalized NEP and phalloidin intensity value of the same ROI was used for the calculation of NEP/phalloidin ratio for the group comparison.

For immunofluorescence of subcelluar NEP, control and HIV-infected MDM on cover slips were prepared as above and fixed with 4% PFA, followed by incubation with 0.5% Triton-X-100 for 15 minutes at room temperature for membrane permeabilization. Then cells were incubated with blocking buffer (0.1% Triton-X-100, 5% BSA and 5% normal donkey serum in PBS) for 1 hour at room temperature. In order to locate NEP at a subcellular level, double immunofluorescence was conducted by co-incubating cells with NEP antibody (1:50; goat polyclonal, R&D Systems) and an antibody for established organelle markers; Heat shock protein 90kDa beta (Grp94), endoplasmic reticulum marker, (1:100, rabbit polyclonal, ab3674, Abcam, Cambridge, MA, USA); Lysosomal-associated membrane protein 1 (LAMP1), lysosomal marker, (1:100, rabbit polyclonal, ab24170, Abcam); GM130, cis-Golgi matrix protein and Golgi apparatus marker, (1:100, rabbit monoclonal, ab52649, Abcam). Subsequently, cells were incubated with appropriate fluorescent-labeled secondary antibodies diluted 1:500 in PBS (for NEP, Alexa Fluor 488 donkey anti-goat IgG; for all three markers, Alexa Fluor 594 donkey anti-rabbit IgG) for 20 minutes at room temperature. Nuclei were stained with Hoechst 33342 (1:1000). Images were acquired using a Zeiss 510 Meta Confocal Laser Scanning Microscope (Carl Zeiss) at an objective of 40X and a 2X zoom view for the interested area.

Statistical tests

Data were presented as means ± standard deviation (SD) unless otherwise noted. All experiments were repeated at least three times with different donors, and all data were evaluated statistically by the analysis of variance (ANOVA), followed by Nweman-Keuls multiple comparison tests using software (Prism 4.0, GraphPad Software, La Jolla, CA, USA). In the case of single mean comparison, data were analyzed by t test. P values < 0.05 was regarded as statistically significant.

Results

HIV reduced Aβ degradation in MDM

We have previously shown that Aβ degradation was reduced in HIV-infected MDM as determined by the clearance of aggregated ^{125}I-Aβ (5). To understand the changes in the clearance of monomeric Aβ, we have developed an experimental model for the clearance of monomeric Aβ after phagocytosis in MDM as described previously (45). Briefly, MDM were infected with HIV-1_{pYu-2} for 24 hours, and at 3dpi the cells were incubated with 10 μM monomeric Aβ42 for 1 hour, 24 hours later cells were then subjected to immunofluorescence of NU-2 for Aβ and Hoechst 33342 for nuclear staining (Figure 1 A-H). The intensity of NU-2 staining was enhanced by viral infection (Figure 1 C and G), consistent with the significant difference as determined by fluorescent intensity measurement (Fig 1 I). These data suggest that monomeric Aβ clearance is reduced in HIV-1-infected MDM.

NEP activity was inhibited by HIV infection of MDM

NEP and IDE are two extensively characterized Aβ degrading enzymes, although their enzyme activities in human MDM have not been well characterized. We have compared the activities of these enzymes in MDM using the fluorogenic peptide Mca-RPPGFSAFK(Dnp)-OH and inhibitors for IDE and NEP (insulin and thiorphan, respectively). NEP showed approximately 4-fold higher endopeptidase activity than IDE in MDM at both days 3 and 7 after M-CSF-treatment (Figure 2), suggesting that NEP is a dominant Aβ degrading enzyme during the monocytic differentiation into MDM. We next examined the effect of viral infection on NEP activity in MDM at 3, 7, and 10 days dpi. NEP endopeptidase activity was significantly decreased by HIV infection by 28.6, 58.4, and 67.6% at 3, 7, and 10 dpi respectively (Figure 3). IDE activity was relatively very low and unchanged by viral infection (data not shown). The infection efficiency was determined by HIV-1 p24 staining of MDM after infection (Figure 4, green), which was 68-100% (average 89%) at 3 dpi and 100% at 7 and 10 dpi, regardless of donors.

To understand the mechanism responsible for reduced NEP activity in HIV-infected-MDM, we have examined the protein expression levels of IDE and NEP by Western blotting. Neither IDE nor NEP protein levels were reduced after HIV infection (Figure 5). This suggests that the alteration in NEP activity is not due to the changes in its expression level, but is potentially due to its post-translational modifications or alterations in its cellular distribution. Since HIV-Tat protein has been shown to inhibit NEP activity (37), we have examined the direct effect of different doses of intact Tat protein (Tat_{1-72}, 0.1 – 10 pg/mL) and gp120 (1-100μM) on the activities of purified recombinant human NEP and IDE proteins *in vitro*. However, neither Tat nor gp120 protein inhibited NEP or IDE activity, ruling out the potential that these proteins directly inhibit the Aβ degrading enzymes (data not shown).

Reduction of cell surface NEP in HIV infected MDM

NEP activity is sensitive to the changes of pH and has maximum activity at neutral pH, suggesting that its distribution on cell surface is critical for its maximum activity as compared to its intracellular distribution in acidic environments, such as endosomes or lysosomes, or endoplasmic reticulum (ER), where trafficking of extracellular peptides are negligible (46). Thus, we have examined if viral infection can alter cellular distribution of NEP and hence its activity. MDM were infected with HIV-$1_{pYu\text{-}2}$ and fixed for immunofluorescence of NEP under both permeabilized and non-permeabilized conditions at 7 dpi (Figure 6). Infection efficiency of the MDM was about 100% as determined by HIV-1 p24 staining. Using an antibody that recognizes the extracellular domain of NEP, we revealed that NEP was prominently expressed on the cell surface in the control group (Figure 6A). However, almost no NEP was detected on the surface of MDM after viral infection (90% inhibition vs. control, Figure 6A-B). On the other hand, cytoplasmic NEP intensity was stronger in HIV-infected MDM when compared with that of the uninfected group (247% increase vs. control, Figure 6A-D). In addition, phalloiding staining (red) representing the F-actin signal was consistent among MDM with or without infection (Figure 5B).

To further understand the redistribution of NEP after viral infection, we performed laser scanning confocal microscopy to detect the co-localization of NEP with organelle markers. In control uninfected MDM, intracellular NEP was mainly co-localized with the ER (GRP94), lysosomes (LAMP1), and to a lesser extent the Golgi apparatus (GM130) (Figure 6). Viral infection of MDM enhanced the cytoplasmic NEP signal intensity relative to the uninfected control group, part of which shows co-localization in the ER and lysosomes (arrows in GRP94 and LAMP1 panels, Figure 7). However, NEP also was found to accumulate in the cytoplasmic organelles other than the either ER or the lysosome, presumably endosomes. These results show that HIV infection dramatically restrained the cell surface expression of NEP, resulting in accumulation of cytoplasmic NEP in the endoplasmic reticulum and lysosomes. This could be due to impaired post-translational modification of NEP at the ER or enhanced endocytosis of cell surface NEP to lysosome due to viral infection, leading to NEP inactivation.

HIV infection inhibited Aβ degradation in microglia

To understand if Aβ clearance is compromised by viral infection in the central nervous system, we have tested if HIV also inhibits degradation of monomeric Aβ in microglia. For that purpose, primary cultured human microglia were infected with HIV-$1_{pYu\text{-}2}$ for 3 days, followed by incubation with different doses of monomeric Aβ and immunofluorescence with anti-Aβ antibody 6E10 after 24-hour incubation. Consistent with the result found in MDM, HIV infection of microglia significantly increased the fluorescent intensity of Aβ at both 1 and 5 μM doses (55 and 132% increase vs. control, respectively), suggesting that reduced Aβ clearance occurs in primary microglia as well (Figure 8A). In accord, NEP activity was also significantly reduced by viral infection at 3 dpi (12% reduction vs. control, Figure 8B), although the difference was much smaller than the one we saw in virus-infected MDM. This suggests that total NEP activity is relatively unchanged and does not directly reflect the reduced Aβclearance in virus-infected microglia, consistent with our finding that the alteration in cellular distribution of NEP plays a role in Aβ clearance as demonstrated in MDM. These data suggest that Aβ clearance and NEP activity are also compromised by HIV infection of human microglia.

Discussion

Understanding the regulation of amyloid clearance in the context of an HIV infection is critical for the prevention of the early onset of senile dementia in affected populations. Perivascular macrophages play an important role in the clearance of Aβ exported from the brain, which might be compromised by HIV viral infection. In this present study, the clearance of monomeric Aβ is significantly inhibited by viral infection of MDM, which express both IDE and NEP as Aβ degrading enzymes. NEP activity is more potent than IDE activity in uninfected, differentiated MDM and the viral infection significantly compromises the enzyme activity as determined by the virus-infected MDM lysates. While the viral infection does not alter the cellular protein expression of NEP or IDE, it greatly reduces the cell surface NEP level. We have shown that HIV infection induces an intracellular re-distribution of NEP primarily to the endoplasmic reticulum and lysosomal compartments. An additional, intracellular compartment of NEP may also include endosomesal compartments considering an internalization mechanism of the enzyme.

Since NEP is a neutral zinc-dependent metalloprotease and its activity is diminished at lower pH or in the absence of zinc (46), either ER, lysosomal, or endosomeal - localized NEP might not have optimal endopeptidase activity. Therefore, HIV infection leading to a redistribution of NEP to intracellular compartments with lower than normal physiologically pH is likely to impair NEP enzyme activity. Indeed, re-distribution of NEP to specific intracellular compartments by fusing recombinant NEP to different organelle-specific molecules results in diminished NEP activity; the wild type NEP has the most enzyme activity whereas the NEP fused to ER-targeting molecule demonstrated the least activity (47). Indeed, it has been reported that PBMC from HIV-1 infected subjects have abnormal cell surface enzyme kinetics (including NEP), and the subcellular distribution of these enzymes were also markedly changed (49). Thus, it is possible that impairment of Aβ clearance at early time points may be attributed to the reduction in cell surface level of NEP (where NEP is situated in optimal pH).

The mechanism of virus-induced re-distribution of NEP is unknown. One possibility is the endocytosis of NEP along with viral infection of MDM. However, so far there is no specific viral capsid or envelop protein reported to interact with NEP for the induction of endocytosis. HIV gp120 had no effect on either purified NEP or IDE activity *in vitro*. Alternatively, NEP may be endocytosed along with viral endocytosis as a bystander membrane protein, effectively inducing the miss-balance of cell surface NEP and recycling/endocytosed NEP after viral infection. HIV-1 Tat can bind to NEP and inhibit its enzyme activity in primary cultured neurons and purified enzyme systems (37, 38). However, intact Tat protein failed to inhibit purified recombinant NEP in our system. Although there is a possibility that Tat protein is partially processed in the cells and has NEP inhibitory activity in MDM, these data suggest that the reduced NEP activity by HIV infection is not due to the direct effect of viral proteins, but could be due to their interaction with NEP for its endocytosis or impairment of post-translational modification of NEP as part of viral suppression mechanisms.

Some post-translational modification of NEP can also be altered by viral infection. An alternative mechanism affecting NEP surface expression is glycosylation, which plays a critical role in regulating transport of NEP to the cell surface as well as the enzymatic activity of NEP (46). Decreased glycosylation results in reduced transport of NEP to the cell surface, thus HIV infection may somehow inhibit the glycosylation level of NEP. Unfortunately, the large bands of the NEP on the immunoblotting data do not allow us to observe molecular weight modifications, precluding from the conclusion. Another possibility lies in that HIV infection enhances endocytosis by viral infection and entry, and

this may then lead to the enhanced relocation of NEP into endosomes (48). However, the detailed mechanisms responsible for disrupting NEP translocation from the plasma membrane by HIV infection remains to be elucidated in future studies.

One caveat of this NEP re-distribution theory is that it does not explain the mechanism of reduced NEP activity in the virus-infected MDM lysate, which is assayed at an optimum pH condition (pH 7.5). HIV-infected cells are in a cellular redox state, which is closely linked to an increased level of ceramide, sphingomyelin, and 4-hydroxynonenal (HNE). These oxidative stress markers were increased in HIV encephalitis (48, 49). It was shown that NEP is modified by HNE adducts, resulting in decreased activity in the brain of AD patients and cultured cells (50-52). Thus, IDE and NEP may undergo oxidation-mediated modifications after viral infection and are therefore inactivated.

In addition, HIV viral infection may also compromise activity of NEP and IDE by virtue of deregulating apolipoprotein E (ApoE), which plays a role in facilitating the proteolytic clearance of soluble Aβ from the brain by NEP and IDE (53). It was reported that in HIV-infected brains, binding of viral Tat protein to (low-density lipoprotein receptor-related protein) LRP resulted in substantial inhibition of neuronal binding, uptake and degradation of physiological ligands for LRP such as ApoE (54). Hence it would be beneficial to examine if there is an alteration of ApoE levels in HIV-infected brains. Additionally, brain ApoE expression may be reduced by HIV infection since it has been shown that HIV downregulates renal ApoE expression (55).

Interestingly, antioxidant or anti-inflammatory supplements could potentially alleviate the oxidation-mediated impairment of NEP activity and enhance Aβ clearance in HIV affected brains. Indeed, it has previously been shown that simavastatin, an anti-inflammatory compound, can attenuate virus-induced Aβ accumulation in brain endothelial cells (56). Taken together, restoration of NEP activity in the brain at the early stages of HIV-associated dementia may represent an effective strategy to prevent or attenuate disease progression.

Finally, it should be noted that viral infection of mononuclear phagocytes induces innate immunity responses, which are characteristic pro-inflammatory activation. This leads to enhanced production of pro-inflammatory cytokines, such as interferon-γ and tumor necrosis factor-α, which enhances production of Aβ through upregulation of amyloid precursor protein (APP) and beta-site APP converting enzyme 1 from neurons and astrocytes (23). Pro-inflammatory cytokines also potently suppress Aβ clearance from human mononuclear phagocytes via down-regulation of Aβ degrading enzymes and chaperone molecules involved in protein refolding (39). Thus, Bystander effect of brain parenchyma activation should be taken into account for understanding the overall mechanism of beta-amyloidosis in brain.

In summary, we demonstrate that monomeric Aβ degradation is reduced by HIV infection of human MDM as early as 3 dpi. This is accompanied by redistribution of cell surface NEP to intracellular compartments at 3 dpi and reduction in NEP activity in cell lysates at 7 dpi without alteration of cellular expression levels of NEP or IDE. Viral Tat or pg120 has no effect on purified IDE or NEP enzyme activity *in vitro*. Comparable results are also found in human primary cultured microglia, suggesting that viral infection also compromises microglial Aβ clearance in the brain. These data suggest that modulation of amyloid clearance by peripheral macrophages is a potential preventative target of Aβ-related cognitive disorders in affected populations.

Acknowledgments

We would like to thank Kathy Estes, Kaitlin Ingraham, and Rob Freilich for manuscript editing, William Klein for NU-1 antibody, and Li Wu for tissue culture.

References

1. Gisslen M, Krut J, Andreasson U, Blennow K, Cinque P, Brew BJ, Spudich S, Hagberg L, Rosengren L, Price RW, Zetterberg H. Amyloid and tau cerebrospinal fluid biomarkers in HIV infection. BMC Neurol. 2009; 9:63. [PubMed: 20028512]
2. Valcour VG, Shikuma CM, Watters MR, Sacktor NC. Cognitive impairment in older HIV-1-seropositive individuals: prevalence and potential mechanisms. AIDS. 2004; 18 1:S79–86. [PubMed: 15075502]
3. Pulliam L. HIV regulation of amyloid beta production. J Neuroimmune Pharmacol. 2009; 4:213–217. [PubMed: 19288202]
4. Esiri MM, Biddolph SC, Morris CS. Prevalence of Alzheimer plaques in AIDS. J Neurol Neurosurg Psychiatry. 1998; 65:29–33. [PubMed: 9667557]
5. Xu J, Ikezu T. The comorbidity of HIV-associated neurocognitive disorders and Alzheimer's disease: a foreseeable medical challenge in post-HAART era. J Neuroimmune Pharmacol. 2009; 4:200–212. [PubMed: 19016329]
6. Green DA, Masliah E, Vinters HV, Beizai P, Moore DJ, Achim CL. Brain deposition of beta-amyloid is a common pathologic feature in HIV positive patients. AIDS. 2005; 19:407–411. [PubMed: 15750394]
7. Guallar JP, Gallego-Escuredo JM, Domingo JC, Alegre M, Fontdevila J, Martinez E, Hammond EL, Domingo P, Giralt M, Villarroya F. Differential gene expression indicates that ‘buffalo hump’ is a distinct adipose tissue disturbance in HIV-1-associated lipodystrophy. AIDS. 2008; 22:575–584. [PubMed: 18316998]
8. Bell RD, Zlokovic BV. Neurovascular mechanisms and blood-brain barrier disorder in Alzheimer's disease. Acta Neuropathol. 2009; 118:103–113. [PubMed: 19319544]
9. Hardy JA, Higgins GA. Alzheimer's disease: the amyloid cascade hypothesis. Science. 1992; 256:184–185. [PubMed: 1566067]
10. Hardy J, Selkoe DJ. The amyloid hypothesis of Alzheimer's disease: progress and problems on the road to therapeutics. Science. 2002; 297:353–356. [PubMed: 12130773]
11. Deane R, Sagare A, Zlokovic BV. The role of the cell surface LRP and soluble LRP in blood-brain barrier Abeta clearance in Alzheimer's disease. Curr Pharm Des. 2008; 14:1601–1605. [PubMed: 18673201]
12. Zlokovic BV. The blood-brain barrier in health and chronic neurodegenerative disorders. Neuron. 2008; 57:178–201. [PubMed: 18215617]
13. Cosenza MA, Zhao ML, Lee SC. HIV-1 expression protects macrophages and microglia from apoptotic death. Neuropathol Appl Neurobiol. 2004; 30:478–490. [PubMed: 15488024]
14. Merrill JE, Chen IS. HIV-1, macrophages, glial cells, and cytokines in AIDS nervous system disease. FASEB J. 1991; 5:2391–2397. [PubMed: 2065887]
15. Lee CY, Landreth GE. The role of microglia in amyloid clearance from the AD brain. J Neural Transm. 2010; 117:949–960. [PubMed: 20552234]
16. Gate D, Rezai-Zadeh K, Jodry D, Rentsendorj A, Town T. Macrophages in Alzheimer's disease: the blood-borne identity. J Neural Transm. 2010; 117:961–970. [PubMed: 20517700]
17. Malm TM, Koistinaho M, Parepalo M, Vatanen T, Ooka A, Karlsson S, Koistinaho J. Bone-marrow-derived cells contribute to the recruitment of microglial cells in response to beta-amyloid deposition in APP/PS1 double transgenic Alzheimer mice. Neurobiol Dis. 2005; 18:134–142. [PubMed: 15649704]
18. Simard AR, Soulet D, Gowing G, Julien JP, Rivest S. Bone marrow-derived microglia play a critical role in restricting senile plaque formation in Alzheimer's disease. Neuron. 2006; 49:489–502. [PubMed: 16476660]

19. Zhao L, Lin S, Bales KR, Gelfanova V, Koger D, Delong C, Hale J, Liu F, Hunter JM, Paul SM. Macrophage-mediated degradation of beta-amyloid via an apolipoprotein E isoform-dependent mechanism. J Neurosci. 2009; 29:3603–3612. [PubMed: 19295164]
20. Blasko I, Veerhuis R, Stampfer-Kountchev M, Saurwein-Teissl M, Eikelenboom P, Grubeck-Loebenstein B. Costimulatory effects of interferon-gamma and interleukin-1beta or tumor necrosis factor alpha on the synthesis of Abeta1-40 and Abeta1-42 by human astrocytes. Neurobiol Dis. 2000; 7:682–689. [PubMed: 11114266]
21. Rossner S, Apelt J, Schliebs R, Perez-Polo JR, Bigl V. Neuronal and glial beta-secretase (BACE) protein expression in transgenic Tg2576 mice with amyloid plaque pathology. J Neurosci Res. 2001; 64:437–446. [PubMed: 11391698]
22. Hartlage-Rubsamen M, Zeitschel U, Apelt J, Gartner U, Franke H, Stahl T, Gunther A, Schliebs R, Penkowa M, Bigl V, Rossner S. Astrocytic expression of the Alzheimer's disease beta-secretase (BACE1) is stimulus-dependent. Glia. 2003; 41:169–179. [PubMed: 12509807]
23. Yamamoto M, Kiyota T, Horiba M, Buescher JL, Walsh SM, Gendelman HE, Ikezu T. Interferon-gamma and tumor necrosis factor-alpha regulate amyloid-beta plaque deposition and beta-secretase expression in Swedish mutant APP transgenic mice. Am J Pathol. 2007; 170:680–692. [PubMed: 17255335]
24. Iwata N, Tsubuki S, Takaki Y, Watanabe K, Sekiguchi M, Hosoki E, Kawashima-Morishima M, Lee HJ, Hama E, Sekine-Aizawa Y, Saido TC. Identification of the major Abeta1-42-degrading catabolic pathway in brain parenchyma: suppression leads to biochemical and pathological deposition. Nat Med. 2000; 6:143–150. [PubMed: 10655101]
25. Iwata N, Tsubuki S, Takaki Y, Shirotani K, Lu B, Gerard NP, Gerard C, Hama E, Lee HJ, Saido TC. Metabolic regulation of brain Abeta by neprilysin. Science. 2001; 292:1550–1552. [PubMed: 11375493]
26. Kurochkin IV, Goto S. Alzheimer's beta-amyloid peptide specifically interacts with and is degraded by insulin degrading enzyme. FEBS Lett. 1994; 345:33–37. [PubMed: 8194595]
27. Carson JA, Turner AJ. Beta-amyloid catabolism: roles for neprilysin (NEP) and other metallopeptidases? J Neurochem. 2002; 81:1–8. [PubMed: 12067222]
28. Eckman EA, Eckman CB. Abeta-degrading enzymes: modulators of Alzheimer's disease pathogenesis and targets for therapeutic intervention. Biochem Soc Trans. 2005; 33:1101–1105. [PubMed: 16246055]
29. Vardy ER, Catto AJ, Hooper NM. Proteolytic mechanisms in amyloid-beta metabolism: therapeutic implications for Alzheimer's disease. Trends Mol Med. 2005; 11:464–472. [PubMed: 16153892]
30. Wang DS, Dickson DW, Malter JS. beta-Amyloid degradation and Alzheimer's disease. J Biomed Biotechnol. 2006; 2006:58406. [PubMed: 17047308]
31. Hama E, Shirotani K, Masumoto H, Sekine-Aizawa Y, Aizawa H, Saido TC. Clearance of extracellular and cell-associated amyloid beta peptide through viral expression of neprilysin in primary neurons. J Biochem. 2001; 130:721–726. [PubMed: 11726269]
32. Tanzi RE, Moir RD, Wagner SL. Clearance of Alzheimer's Abeta peptide: the many roads to perdition. Neuron. 2004; 43:605–608. [PubMed: 15339642]
33. Hickman SE, Allison EK, El Khoury J. Microglial dysfunction and defective beta-amyloid clearance pathways in aging Alzheimer's disease mice. J Neurosci. 2008; 28:8354–8360. [PubMed: 18701698]
34. El-Amouri SS, Zhu H, Yu J, Marr R, Verma IM, Kindy MS. Neprilysin: an enzyme candidate to slow the progression of Alzheimer's disease. Am J Pathol. 2008; 172:1342–1354. [PubMed: 18403590]
35. Farris W, Schutz SG, Cirrito JR, Shankar GM, Sun X, George A, Leissring MA, Walsh DM, Qiu WQ, Holtzman DM, Selkoe DJ. Loss of neprilysin function promotes amyloid plaque formation and causes cerebral amyloid angiopathy. Am J Pathol. 2007; 171:241–251. [PubMed: 17591969]
36. Dorfman VB, Pasquini L, Riudavets M, Lopez-Costa JJ, Villegas A, Troncoso JC, Lopera F, Castano EM, Morelli L. Differential cerebral deposition of IDE and NEP in sporadic and familial Alzheimer's disease. Neurobiol Aging. 2010; 31:1743–1757. [PubMed: 19019493]

37. Rempel HC, Pulliam L. HIV-1 Tat inhibits neprilysin and elevates amyloid beta. AIDS. 2005; 19:127–135. [PubMed: 15668537]
38. Daily A, Nath A, Hersh LB. Tat peptides inhibit neprilysin. J Neurovirol. 2006; 12:153–160. [PubMed: 16877296]
39. Yamamoto M, Kiyota T, Walsh SM, Liu J, Kipnis J, Ikezu T. Cytokine-mediated inhibition of fibrillar amyloid-beta peptide degradation by human mononuclear phagocytes. J Immunol. 2008; 181:3877–3886. [PubMed: 18768842]
40. Gendelman HE, Orenstein JM, Martin MA, Ferrua C, Mitra R, Phipps T, Wahl LA, Lane HC, Fauci AS, Burke DS, et al. Efficient isolation and propagation of human immunodeficiency virus on recombinant colony-stimulating factor 1-treated monocytes. J Exp Med. 1988; 167:1428–1441. [PubMed: 3258626]
41. Borgmann K, Gendelman HE, Ghorpade A. Isolation and HIV-1 infection of primary human microglia from fetal and adult tissue. Methods Mol Biol. 2005; 304:49–70. [PubMed: 16061966]
42. Chao CC, Gekker G, Hu S, Peterson PK. Human microglial cell defense against Toxoplasma gondii. The role of cytokines. J Immunol. 1994; 152:1246–1252. [PubMed: 8301129]
43. Li Y, Kappes JC, Conway JA, Price RW, Shaw GM, Hahn BH. Molecular characterization of human immunodeficiency virus type 1 cloned directly from uncultured human brain tissue: identification of replication-competent and -defective viral genomes. J Virol. 1991; 65:3973–3985. [PubMed: 1830110]
44. Xu J, Tsutsumi K, Tokuraku K, Estes KA, Hisanaga SI, Ikezu T. Actin interaction and regulation of cyclin-dependent kinase 5/p35 complex activity. J Neurochem. 2010
45. Kiyota T, Yamamoto M, Xiong H, Lambert MP, Klein WL, Gendelman HE, Ransohoff RM, Ikezu T. CCL2 accelerates microglia-mediated Abeta oligomer formation and progression of neurocognitive dysfunction. PLoS One. 2009; 4:e6197. [PubMed: 19593388]
46. Barros NM, Campos M, Bersanetti PA, Oliveira V, Juliano MA, Boileau G, Juliano L, Carmona AK. Neprilysin carboxydipeptidase specificity studies and improvement in its detection with fluorescence energy transfer peptides. Biol Chem. 2007; 388:447–455. [PubMed: 17391066]
47. Hama E, Shirotani K, Iwata N, Saido TC. Effects of neprilysin chimeric proteins targeted to subcellular compartments on amyloid beta peptide clearance in primary neurons. J Biol Chem. 2004; 279:30259–30264. [PubMed: 15100223]
48. Miyauchi K, Kim Y, Latinovic O, Morozov V, Melikyan GB. HIV enters cells via endocytosis and dynamin-dependent fusion with endosomes. Cell. 2009; 137:433–444. [PubMed: 19410541]
49. Leoni LM, Losa GA. Changes in membrane enzymes and glycosphingolipids in lymphocytes from HIV-1--infected and noninfected intravenous drug users. J Acquir Immune Defic Syndr Hum Retrovirol. 1996; 11:188–197. [PubMed: 8556402]
50. Wang R, Malter JS, Wang DS. N-acetylcysteine prevents 4-hydroxynonenal- and amyloid-beta-induced modification and inactivation of neprilysin in SH-SY5Y cells. J Alzheimers Dis. 2010; 19:179–189. [PubMed: 20061637]
51. Wang DS, Iwata N, Hama E, Saido TC, Dickson DW. Oxidized neprilysin in aging and Alzheimer's disease brains. Biochem Biophys Res Commun. 2003; 310:236–241. [PubMed: 14511676]
52. Shinall H, Song ES, Hersh LB. Susceptibility of amyloid beta peptide degrading enzymes to oxidative damage: a potential Alzheimer's disease spiral. Biochemistry. 2005; 44:15345–15350. [PubMed: 16285738]
53. Jiang Q, Lee CY, Mandrekar S, Wilkinson B, Cramer P, Zelcer N, Mann K, Lamb B, Willson TM, Collins JL, Richardson JC, Smith JD, Comery TA, Riddell D, Holtzman DM, Tontonoz P, Landreth GE. ApoE promotes the proteolytic degradation of Abeta. Neuron. 2008; 58:681–693. [PubMed: 18549781]
54. Liu Y, Jones M, Hingtgen CM, Bu G, Laribee N, Tanzi RE, Moir RD, Nath A, He JJ. Uptake of HIV-1 tat protein mediated by low-density lipoprotein receptor-related protein disrupts the neuronal metabolic balance of the receptor ligands. Nat Med. 2000; 6:1380–1387. [PubMed: 11100124]
55. Arora S, Husain M, Kumar D, Patni H, Pathak S, Mehrotra D, Reddy VK, Reddy LR, Salhan D, Yadav A, Mathieson PW, Saleem MA, Chander PN, Singhal PC. Human immunodeficiency virus

downregulates podocyte apoE expression. Am J Physiol Renal Physiol. 2009; 297:F653–661. [PubMed: 19553347]

56. Andras IE, Eum SY, Huang W, Zhong Y, Hennig B, Toborek M. HIV-1-induced amyloid beta accumulation in brain endothelial cells is attenuated by simvastatin. Mol Cell Neurosci. 2010; 43:232–243. [PubMed: 19944163]

Abbreviations

AD	Alzheimer's disease
A®	amyloid-β peptide
APP	amyloid precursor protein
ART	antiretroviral therapy
ApoE	apolipoprotein E
CNS	central nervous system
ER	endoplasmic reticulum
GRP94	Heat shock protein 90kDa beta
HAART	highly active antiretroviral therapy
HFIP	hexafluoro-2-propanol
HNE	4-hydroxynonenal
IDE	insulin-degrading enzyme
LAMP1	Lysosomal-associated membrane protein 1
LRP	low-density lipoprotein receptor-related protein
MDM	monocyte-derived macrophages
MMP	metalloprotease
NEP	neprilysin
PFA	paraformaldehyde
SRA	scavenger receptor A

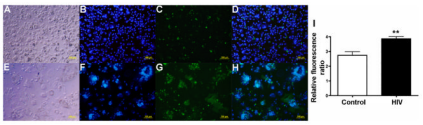

Figure 1. Impaired clearance of phagocytosed monomeric Aβ in HIV-1 infected MDM

Primary cultured MDM were plated onto poly-D-lysine-coated 96-well plates (black walled for fluorescence measurement). MDM remained as uninfected (**A-D**) or infected with HIV-1_{pYU-2} for 24 hours (**E-H**). 3 days later, cells were pulsed with monomeric Aβ42 (10μM) for 1 hour. Unbound Aβ was washed away and cells were fixed 4% paraformaldehyde after 24 hours. Immunofluorescence was conducted with Aβ-specific NU-2 mAb (green, **C-D, G-H**) and Hoechst 33342 for nuclear staining (blue, **B, D, F, H**). **A** and **E**, phase contrast images. **D** and **H**, merged images of **B-C** and **F-G**, respectively. Scale bar, 100 μm. **I**, Quantification of Aβ intensity was shown as Aβ/Hoechst 33342 fluorescence intensity % ratio (n=4 per group). ** denotes $p<0.01$ vs. Control group as determined by Student's t-test.

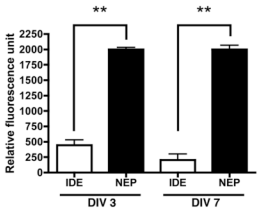

Figure 2. Comparison of IDE and NEP activities in MDM

Human monocytes were differentiated to MDM with M-CSF for 3 or 7 days, and cell lysates were collected for enzymatic assay with a fluorogenic substrate. Insulin (10 μM) or thiorphan (10 μM) was added into the reaction system to detect the IDE or NEP activity and the results were shown as shown as relative fluorescence units at 3 and 7 days of differentiation in vitro (DIV). ** denotes $p<0.01$ vs. control group as determined by t-test.

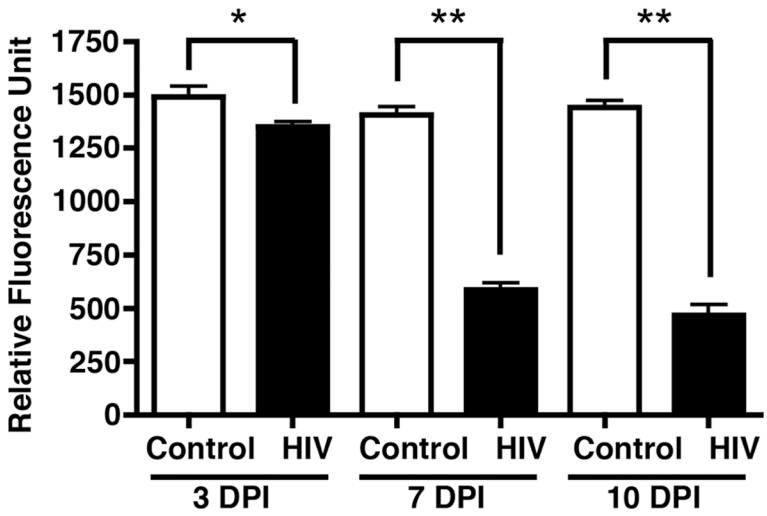

Figure 3. HIV-1 infection reduced NEP activity in MDM

Human MDM (2×10^6 cells/well in 6-well plates) were infected (HIV group) or uninfected (Control group) with HIV-1_{pYu2}, incubated for 3, 7, or 10 days, and cell lysates were collected for immunoprecipitation and NEP activity determination shown as relative fluorescence units at 3, 7, and 10 days post infection (DPI). * denotes $p < 0.05$, and ** denotes $p<0.01$ by t-test assay.

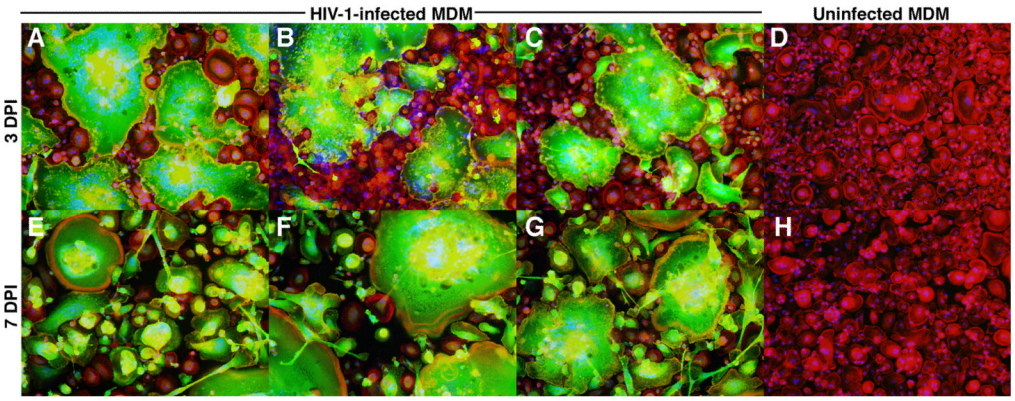

Figure 4. HIV-1 infection of MDM

Human MDM were infected with HIV-1_{pYu2} and fixed at 3 and 7 dpi, followed by immunofluorescence for HIV-1 p24 (green), phalloidin (red, staing F-actin), and Hoechst 33342 (blue, nuclear staining). (A-C), MDM at 3 dpi from different donors; (D), sham-infected MDM at 3 dpi; (E-G), MDM at 7 dpi different donors; (H), sham-infected MDM at 7 dpi.

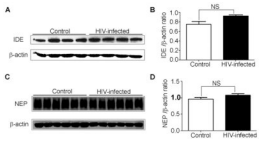

Figure 5. HIV infection did not alter the expression of IDE/NEP in MDM

Cell lysates (25 μg/lane) from MDM with and without HIV-1 $_{pYu2}$ infection were subjected to SDS-PAGE and immunoblotting with anti-IDE (A), anti-NEP (C), or anti-β-actin control (A, C). B and D showed the quantitative comparisons of the IDE or NEP intensities between the control group and HIV group, respectively. NS denotes no statistical difference.

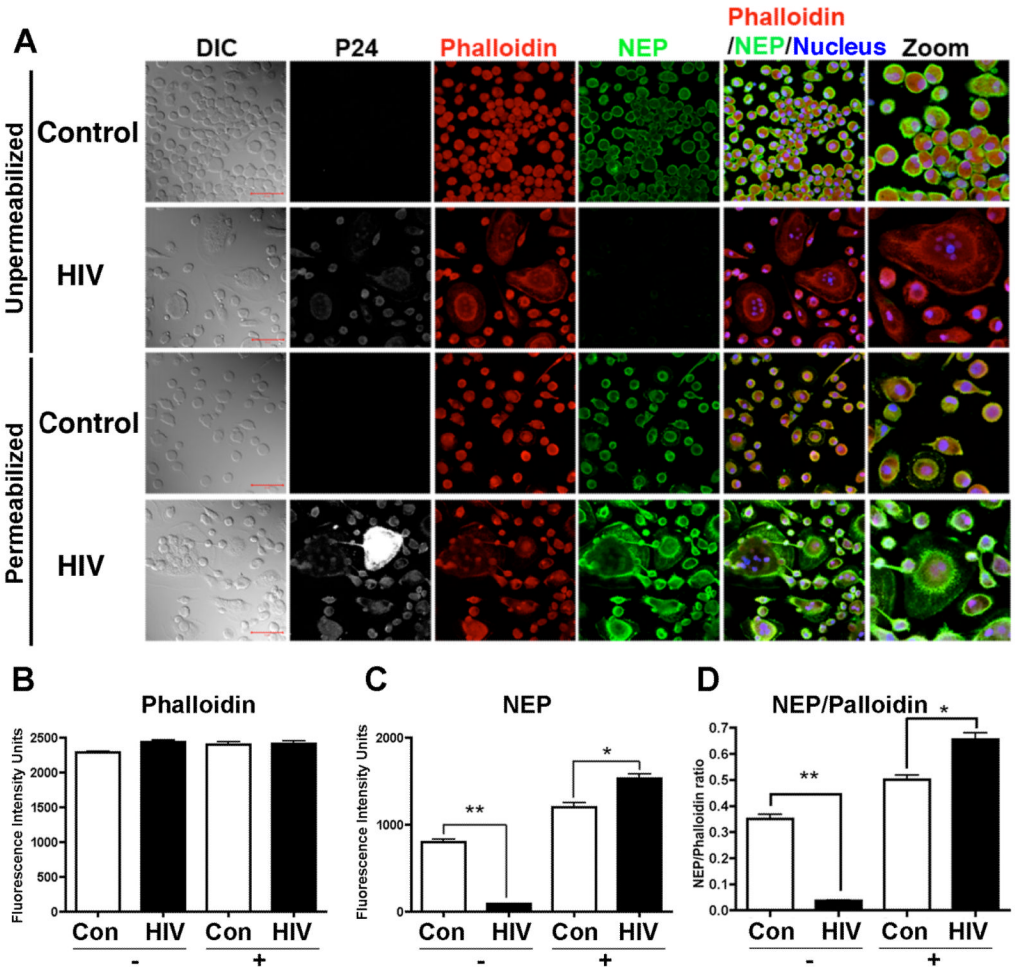

Figure 6. Confocal imaging of plasma membrane-localized and cellular NEPP in MDM

(A) Human MDM (2×10^5 cells/cover slip in 24-well plates) were infected with HIV-1_{pYu2} (HIV group) or with culture medium only (Control group) for 24 hours. Cells were fixed with 4% PFA at 7 dpi. Immunocytochemistry was carried without permeabilization to visualize surface-localized NEP (green) or permeabilization with 0.5% Triton-X-100 to stain intracellular NEP, followed by permeabilization and immunostaining of HIV-1 p24 (white), phalloidin (red), and Hoechst 33342 (blue). (B-D) Average immunofluorescent intensity per region of interest (ROI) was quantified for phalloidin (B), NEP (C), and NEP/phalloidin fluorescent intensity % ratio (n=15 per group). * and ** denotes $p < 0.05$ and 0.01 vs. Control group as determined by ANOVA and Turkey post hoc.

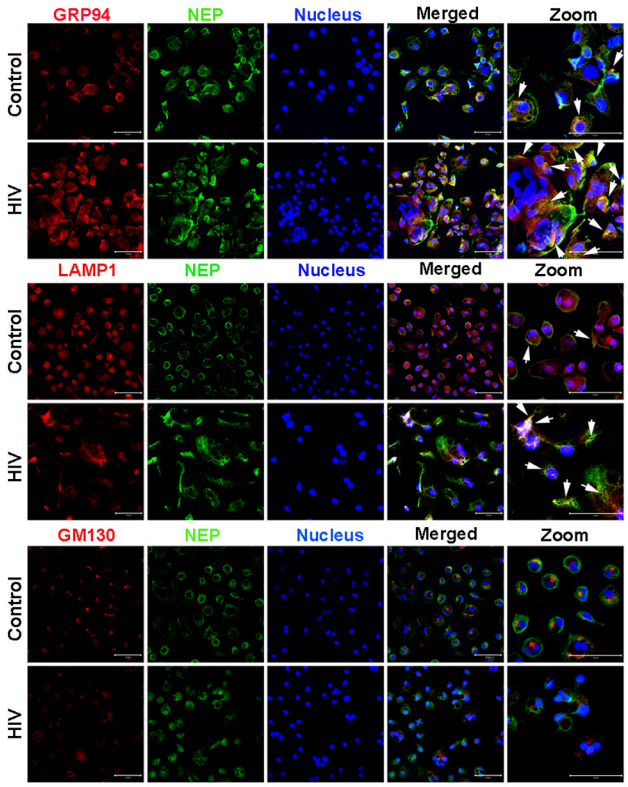

Figure 7. Laser-scanning Confocal Miscroscopy imaging of subcelluar NEP in MDM

Control and HIV-infected MDM were prepared on coverslips, fixed with 4% PFA, and permeabilized with 0.5% Triton-X-100. Then cells were immunostained with anti-NEP (green) plus anti-GRP94, anti-LAMP1, and anti-GM130 (red), which are organellar markers. Nuceli were visualized with Hoechst 33342 (blue). Images were taken with a confocal microscope at an objective of 40× and 2× zoom view for the regions of interest. Arrows indicate co-localized staining between red and green.

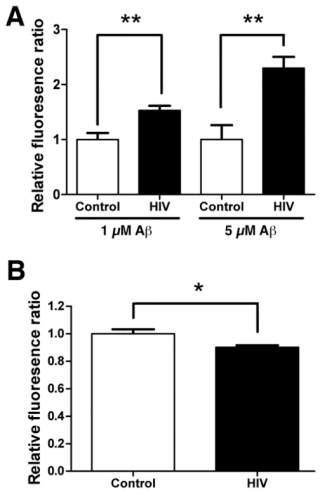

Figure 8. HIV-1 infection reduced Aβ degradation and NEP activity in microglia

(A) Human microglia (5×10^4 cells/well in 96-well plates) were infected (HIV group) or uninfected (Control group) with HIV-1_{pYu2} for three days, and tested for Aβ42 degradation at 1 and 5 uM concentrations as described in Fig. 1. The cells were subjected to immunofluorescence with anti-Aβ antibody (6E10) and Hoechst33342 for flurolometric quantification of Aβ oligomer fluorescent signal (Ex/Em=488 nm/519 nm) which was normalized by the nuclear staining signal (Ex/Em=350 nm/461 nm, n=5 per group). The results were presented as relative fluorescence ratio. * denotes $p < 0.01$ by t-test. (B) Human microglia (1×10^6 cells/well in 6-well plates) were infected (HIV group) or uninfected (Control group) with HIV-1_{pYu2} for three days, and cell lysates were collected for NEP activity determination shown as relative fluorescent units. * denotes $p < 0.05$ by Student's t-test assay.